Nano-Pico Satellite Actuator Fault Diagnosis Based on Adaptive Observer

IOP Conf. Series: Materials Science and Engineering **608** (2019) 012041 doi:10.1088/1757-899X/608/1/012041

Nano-Pico Satellite Actuator Fault Diagnosis Based on Adaptive Observer

Y Fei[1], T Meng[1] and Z H Jin[1]

[1]School of Aeronautics and Astronautics, Zhejiang University, Hangzhou, 310027, China

mengtao@zju.edu.cn

Abstract. This paper concerns with actuators fault diagnosis of nano-pico satellite, and a double adaptive estimation algorithm is proposed. Based on the non-linear mathematical model of reaction flywheel, a parameterized description method of flywheel fault type is established. Using the input and output information of the flywheel, a local adaptive observer is constructed and can identify the fault type of the flywheel. A global adaptive observer based on the satellite dynamics model uses the gyroscope sampling signal and the estimation of local observer as inputs, so failure moment of the other actuator can be identified. Combining two observers' identification results, the fault diagnosis of flywheel and the other actuator can be completed. In this paper, a control system composed of reaction flywheel and magnetorquer is simulated. Results show the effectiveness of proposed method for nano-pico satellite actuator fault diagnosis.

1. Introduction

Nano-Pico satellite denotes the small satellite with mass is ranging from a few kilograms to tens of kilograms and based on microelectronics and micromechanical technology. Due to the constraints of size, weight and power consumption, nano-pico satellite cannot improve its reliability by using the redundant backup method of traditional satellite. Once the failure occurs, the entire space mission will be directly affected.

In the on-orbit failures of spacecraft that have been disclosed abroad, the attitude control subsystem and the power subsystem have the highest failure ratio [1-2]. Attitude control subsystem contains many sensors and actuators, and integrates a variety of algorithms. Focusing on the actuator faults, fault diagnosis methods for spacecraft actuators can be divided into three categories [3-5].

The first is based on the analytical model method, using software redundancy instead of hardware redundancy to obtain residuals, and processing the residuals to achieve detection. In [6], an adaptive observer was proposed for reaction flywheels, which realized the identification of flywheel gain and constant friction moment.

Second, detection methods based on signal processing analyze the measurement signal directly, and extract the characteristics of spectrum, amplitude and variance to achieve fault detection. These methods do not need mathematical model and have strong adaptability. In [7], the wavelet transform is used to analyze the flywheel speed, and the detection of the stalling fault is realized. Vertex principal component analysis (VPCA) was applied to realize fault detection and isolation of actuators in [8-9].

The third methods are based on artificial intelligence, which do not need precise mathematical model. At present, these researches are the most popular, and indicate the direction of the development of autonomous detection in the future. Fault detection of flywheel was realized by using neural network in [10-11].

In summary, the existing research methods are mostly directed to the fault detection of single actuator, and some algorithms have heavy computing burden. In this paper, an adaptive identification algorithm is proposed. The local adaptive observer is designed by using the input and output information of the flywheel. Combined with the dynamic equation, the global observer is designed by using the output information of the gyroscope, and the local observer identification result is taken as input. This can identify the fault torque that does not contain the flywheel fault, thus achieving fault isolation and identification of the actuator. This scheme adapts to the control combination of the flywheel with any other actuator and does not require the establishment of a mathematical model of another actuator.

2. Attitude control system fault analysis

The Attitude Control System (ACS) is the key to ensure the stability of the satellite attitude and the realization of the satellite function. This paper takes the control system composed of the magnetorquer and the reaction flywheel group.

2.1. Flywheel failures

The common faults of the flywheel can be divided into three categories: abnormal torque output, which is caused by increased bearing temperature and poor lubrication, which lead to the increase of friction torque and the decrease of reaction wheel gain efficiency. The idling fault refers to that reaction wheel cannot respond to the normal control torque command due to certain factors, the rotation speed remains almost constant (slowly decreases under the action of friction), the output torque is almost zero; the stalling fault refers to the situation that the output torque of reaction wheel rapidly turns to zero after a huge reverse disturbance is generated.

Consider single reaction flywheel mathematical model:

$$\dot{w}_{\mathrm{w}} = J_{\mathrm{w}}^{-1}\left(kT - vw_{\mathrm{w}} + \mathrm{sgn}\left(w_{\mathrm{w}}\right)T_{\mathrm{fc}}\right) \tag{1}$$

Where w_w denotes the angular velocity of the flywheel; J_{w} is the rotational inertia of each flywheel; k denotes output gain; v is viscous friction coefficient; T denotes command input; T_{fc} is friction moment.

In combination with the flywheel model, its fault can be described by the change of the gain k and the viscous friction coefficient v. v_{f} is the normal viscous friction coefficient.

Table 1. Flywheel fault mode and its parameterized description.

fault mode	k	v
idling	k=0	$v<v_{\mathrm{f}}$
stalling	k=0	$v>v_{\mathrm{f}}$
gain decrease	k<1	-

2.2. Magnetorquer failures

The magnetorquer is mainly composed of a magnetic bar and a drive control circuit. In the time domain, its faults can be divided into: sudden fault, gradual fault and intermittent fault. A sudden fault refers to sudden damage to the hardware, resulting in a large continuous deviation between the output torque and the target value; the gradual failure is due to component wear aging, and the performance slowly decreases with time; the intermittent fault is caused by component aging and poor contact, it is instantaneous sudden change[12].

3. FDI design based on parameter adaptation

Using the output information of the flywheel to design an adaptive observer, the parameters of the flywheel can be identified. The flywheel fault mode can be determined according to Table 1. The global adaptive observer can be designed by using the output information of the gyroscope, and the actual output torque of the flywheel is calculated by using the parameter identification result, use it as the input information of the global sensor, the global identification result only contains the fault torque of the magnetic torque device, and can estimate the fault condition of the magnetic torque device. The algorithm flowchart is shown in Fig.1:

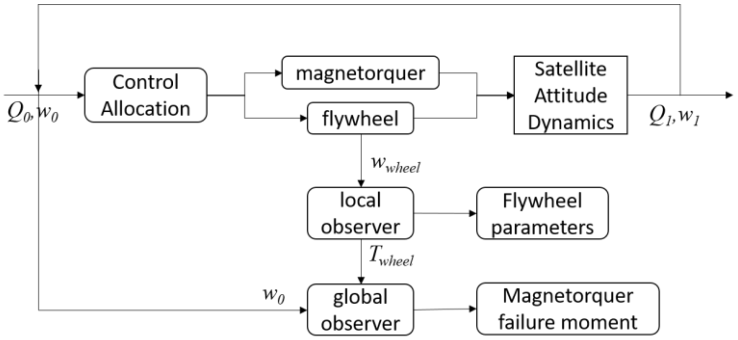

Figure 1. Algorithm flowchart.

3.1. Local parameter adaptive algorithm

The following adaptive observer is designed according to the mathematical model of the flywheel:

$$\dot{\hat{w}}_{\mathrm{w}} = J_{\mathrm{w}}^{-1}\left(\hat{k}T - \hat{v}\hat{w}_{\mathrm{w}} + \mathrm{sgn}\left(\hat{w}_{\mathrm{w}}\right)T_{\mathrm{fc}}\right) + L\left(w_{\mathrm{w}} - \hat{w}_{\mathrm{w}}\right) \tag{2}$$

Where $\hat{w}_{\mathrm{w}}$ denotes the observer state variable, and observer gain L>0.

Define the following variables:

$$\begin{aligned} &\hat{\mathrm{T}}_{\mathrm{wheel}}^{\mathrm{i}} = J_{\mathrm{w}}\left(\hat{w}_{\mathrm{w1}}^{\mathrm{j}} - \hat{w}_{\mathrm{w0}}^{\mathrm{j}}\right) \\ &\tilde{w}_{\mathrm{w}} = w_{\mathrm{w}} - \hat{w}_{\mathrm{w}}, \tilde{k} = k - \hat{k}, \tilde{v} = v - \hat{v} \end{aligned} \tag{3}$$

Given the output gain k and viscous friction coefficient v are positive constant under normal circumstances, we can obtain that:

$$\dot{\tilde{k}} = -\dot{\hat{k}}, \dot{\tilde{v}} = -\dot{\hat{v}} \tag{4}$$

From (1) and (2), the error function describes as:

$$\dot{\tilde{w}}_{\mathrm{w}} = J_{\mathrm{w}}^{-1}\left(\tilde{k}T - vw_{\mathrm{w}} + \hat{v}\hat{w}_{\mathrm{w}} - L\tilde{w}_{\mathrm{w}}\right) \tag{5}$$

The adaptive parameter estimation algorithms are designed as follows:

$$\dot{\hat{k}} = \tau_1 J_{\mathrm{w}}^{-1} T\tilde{w}_{\mathrm{w}}, \dot{\hat{v}} = -\tau_2 J_{\mathrm{w}}^{-1}\hat{w}_{\mathrm{w}}\tilde{w}_{\mathrm{w}} \tag{6}$$

Proof: Consider the following Lyapunov function

$$V = \frac{1}{2}\tilde{w}_{\mathrm{w}}^2 + \frac{1}{2\tau_1}\tilde{k}^2 + \frac{1}{2\tau_2}\tilde{v}^2 \tag{7}$$

From (5) and (6), differentiating function (7) with respect to time yields:

$$\begin{aligned} \dot{V} &= \tilde{w}_{\mathrm{w}}\dot{\tilde{w}}_{\mathrm{w}} + \frac{1}{\tau_1}\tilde{k}\dot{\tilde{k}} + \frac{1}{\tau_2}\tilde{v}\dot{\tilde{v}} \\ &= J_{\mathrm{w}}^{-1}\left(\tilde{k}T - vw_{\mathrm{w}} + \hat{v}\hat{w}_{\mathrm{w}} - L\tilde{w}_{\mathrm{w}}\right)\tilde{w}_{\mathrm{w}} - \frac{1}{\tau_1}\tilde{k}\dot{\hat{k}} - \frac{1}{\tau_2}\tilde{v}\dot{\hat{v}} \\ &= J_{\mathrm{w}}^{-1}\left(-v - L\right)\tilde{w}_{\mathrm{w}}^2 - J_{\mathrm{w}}^{-1}\tilde{v}\hat{w}_{\mathrm{w}}\tilde{w}_{\mathrm{w}} + J_{\mathrm{w}}^{-1}\tilde{k}T\tilde{w}_{\mathrm{w}} - \frac{1}{\tau_1}\tilde{k}\dot{\hat{k}} - \frac{1}{\tau_2}\tilde{v}\dot{\hat{v}} \\ &= -J_{\mathrm{w}}^{-1}\left(v + L\right)\tilde{w}_{\mathrm{w}}^2 \end{aligned} \tag{8}$$

Because v and L are positive constant, one can obtain that $\dot{V} \le 0$, which means that $(\hat{w}_w, \hat{k}, \hat{v})$ asymptotically converges to the true values according to Lyapunov stability theory.

3.2. Global fault adaptive algorithm

Consider the following satellite dynamic function:

$$\dot{\mathbf{w}} = \mathbf{J}^{-1}\left\{\mathbf{I}\mathbf{w}\times\mathbf{w} + \mathbf{C}_w\mathbf{h}\times\mathbf{w} + \mathbf{T}_m + \hat{\mathbf{T}}_{wheel} + \mathbf{T}_{d0} + \mathbf{f}_a\right\}. \tag{9}$$

Where the state $\mathbf{w} \in R^3$ is the satellite angular velocity; $\mathbf{J} \in R^{3\times3}$ is the inertia matrix of the satellite; $\mathbf{C}_w \in R^{3\times4}$ denotes the transformation matrix of the reaction flywheels; $\mathbf{h} \in R^4$ is the reaction flywheel momentum; $\mathbf{T}_m \in R^3$ is the control torque of magnetorquer; $\mathbf{T}_{d0} \in R^3$ is external disturbances; $\mathbf{f}_a \in R^3$ denotes fault moment; $\mathbf{T}_{wheel} \in R^3$ is the estimated output torque of the flywheels.

Define:

$$\begin{aligned} &g(\mathbf{w}) = \mathbf{J}^{-1}\left(\mathbf{I}\mathbf{w}\times\mathbf{w} + \mathbf{C}_w\mathbf{h}\times\mathbf{w}\right)\\ &\mathbf{u} = \mathbf{T}_m + \hat{\mathbf{T}}_{wheel}\\ &\mathbf{B} = \mathbf{J}^{-1}\\ &\mathbf{T}_d = \mathbf{J}^{-1}\mathbf{T}_{d0} \end{aligned} \tag{10}$$

Substituting (10) into (9), it can be derived that:

$$\dot{\mathbf{w}} = g(\mathbf{w}) + \mathbf{B}\mathbf{u} + \mathbf{B}\mathbf{f}_a + \mathbf{T}_d \tag{11}$$

Assumption 1: $g(\mathbf{w})$ satisfies the criterion of Lipschitz, and given a scalar $r > 0$,one can obtain that

$$\left\|g(\mathbf{w}_1) - g(\mathbf{w}_2)\right\| \le r\left\|\mathbf{w}_1 - \mathbf{w}_2\right\| \tag{12}$$

Design the following adaptive observer:

$$\begin{aligned} &\dot{\hat{\mathbf{w}}} = g(\hat{\mathbf{w}}) + \mathbf{B}\mathbf{u} + \mathbf{B}\hat{\mathbf{f}}_a + \mathbf{L}(\mathbf{y} - \hat{\mathbf{y}})\\ &\hat{\mathbf{y}} = \mathbf{C}\hat{\mathbf{w}} \end{aligned} \tag{13}$$

Where $\hat{\mathbf{w}}$ denotes the observer state vector, and observer gain matrix $\mathbf{L}$ is positive definite.

Denote

$$\mathbf{e} = \mathbf{w} - \hat{\mathbf{w}}, \tilde{\mathbf{f}}_a = \mathbf{f}_a - \hat{\mathbf{f}}_a \tag{14}$$

Then the error differentiating function is described by

$$\dot{\mathbf{e}} = g(\mathbf{w}) - g(\hat{\mathbf{w}}) + \mathbf{B}\left(\mathbf{f}_a - \hat{\mathbf{f}}_a\right) + \mathbf{T}_d - \mathbf{L}\mathbf{C}\mathbf{e} \tag{15}$$

Lemma 1 [13]**:** Given a scalar $\mu > 0$ and a symmetric positive definite matrix $\mathbf{Q}$, the following inequality holds:

$$2\mathbf{x}^T\mathbf{y} \le \frac{1}{\mu}\mathbf{x}^T\mathbf{Q}\mathbf{x} + \mu\mathbf{y}^T\mathbf{Q}^{-1}\mathbf{y} \qquad \mathbf{x},\mathbf{y} \in R^n \tag{16}$$

Lemma 2[14]: Given a symmetric positive definite matrix $\mathbf{P}$, the following inequality holds:

$$2\mathbf{e}^T\mathbf{P}\left[g(\mathbf{w}) - g(\hat{\mathbf{w}})\right] \le r^2\mathbf{e}^T\mathbf{P}\mathbf{P}\mathbf{e} + \mathbf{e}^T\mathbf{e} \tag{17}$$

The adaptive fault estimation algorithms are designed as follows:

$$\begin{aligned} &\dot{\hat{\mathbf{f}}}_a = \mathbf{G}\mathbf{F}(\mathbf{y} - \hat{\mathbf{y}}) - \mathbf{T}\mathbf{G}\hat{\mathbf{f}}_a\\ &\mathbf{F}\mathbf{C} = \mathbf{B}^T\mathbf{P} \end{aligned} \tag{18}$$

Where $\mathbf{G}$ and $\mathbf{T}$ are rate matrixes.

Proof: Choose the following Lyapunov function:

$$V = \mathbf{e}^T\mathbf{P}\mathbf{e} + \tilde{\mathbf{f}}_a^T\mathbf{G}^{-1}\tilde{\mathbf{f}}_a^T > 0 \tag{19}$$

Differentiating function (19) with respect to time, one can obtain that:

$$\begin{aligned}\dot{V} &= 2\dot{\mathbf{e}}^{\mathrm{T}}\mathbf{P}\mathbf{e} + 2\dot{\tilde{\mathbf{f}}}_{\mathrm{a}}^{\mathrm{T}}\mathbf{G}^{-1}\tilde{\mathbf{f}}_{\mathrm{a}} \\ &= \mathbf{e}^{\mathrm{T}}\left[(-\mathbf{LC})^{\mathrm{T}}\mathbf{P} + \mathbf{P}(-\mathbf{LC})\right]\mathbf{e} + 2\left[g(\mathbf{w}) - g(\hat{\mathbf{w}})\right]^{\mathrm{T}}\mathbf{P}\mathbf{e} \\ &+2\mathbf{T}_{\mathrm{d}}^{\mathrm{T}}\mathbf{P}\mathbf{e} + 2\left[\mathbf{B}\left(\mathbf{f}_{\mathrm{a}} - \hat{\mathbf{f}}_{\mathrm{a}}\right)\right]^{T}\mathbf{P}\mathbf{e} + 2\dot{\tilde{\mathbf{f}}}_{\mathrm{a}}^{\mathrm{T}}\mathbf{G}^{-1}\tilde{\mathbf{f}}_{\mathrm{a}} \\ &\le \mathbf{e}^{\mathrm{T}}\left[(-\mathbf{LC})^{\mathrm{T}}\mathbf{P} + \mathbf{P}(-\mathbf{LC})\right]\mathbf{e} + r^2\mathbf{e}^{\mathrm{T}}\mathbf{P}\mathbf{P}\mathbf{e} + \mathbf{e}^{\mathrm{T}}\mathbf{e} + 2\mathbf{T}_{\mathrm{d}}^{\mathrm{T}}\mathbf{P}\mathbf{e} \\ &+2\left[\mathbf{B}\left(\mathbf{f}_{\mathrm{a}} - \hat{\mathbf{f}}_{\mathrm{a}}\right)\right]^{\mathrm{T}}\mathbf{P}\mathbf{e} + 2\tilde{\mathbf{f}}_{\mathrm{a}}^{\mathrm{T}}\mathbf{G}^{-1}\left(\dot{\mathbf{f}}_{\mathrm{a}} - \dot{\hat{\mathbf{f}}}_{\mathrm{a}}\right) \\ &\le \mathbf{e}^{\mathrm{T}}\left[(-\mathbf{LC})^{\mathrm{T}}\mathbf{P} + \mathbf{P}(-\mathbf{LC})\right]\mathbf{e} + r^2\mathbf{e}^{\mathrm{T}}\mathbf{P}\mathbf{P}\mathbf{e} + \mathbf{e}^{\mathrm{T}}\mathbf{e} + 2\mathbf{T}_{\mathrm{d}}^{\mathrm{T}}\mathbf{P}\mathbf{e} \\ &+2\left(\mathbf{B}\tilde{\mathbf{f}}_{\mathrm{a}}\right)^{\mathrm{T}}\mathbf{P}\mathbf{e} + 2\tilde{\mathbf{f}}_{\mathrm{a}}^{\mathrm{T}}\mathbf{G}^{-1}\left(\dot{\mathbf{f}}_{\mathrm{a}} - \mathbf{GFCe} + \mathbf{TG}\hat{\mathbf{f}}_{\mathrm{a}}\right) \\ &= \mathbf{e}^{\mathrm{T}}\left[(-\mathbf{LC})^{\mathrm{T}}\mathbf{P} + \mathbf{P}(-\mathbf{LC})\right]\mathbf{e} + r^2\mathbf{e}^{\mathrm{T}}\mathbf{P}\mathbf{P}\mathbf{e} + \mathbf{e}^{\mathrm{T}}\mathbf{e} \\ &+2\mathbf{T}_{\mathrm{d}}^{\mathrm{T}}\mathbf{P}\mathbf{e} + \left[2\tilde{\mathbf{f}}_{\mathrm{a}}^{\mathrm{T}}\mathbf{G}^{-1}\dot{\mathbf{f}}_{\mathrm{a}} + 2\tilde{\mathbf{f}}_{\mathrm{a}}^{\mathrm{T}}\mathbf{G}^{-1}\mathbf{TG}\hat{\mathbf{f}}_{\mathrm{a}}\right]\end{aligned} \tag{20}$$

From Lemma 1, one can obtain the following inequalities:

$$2\mathbf{T}_d^T\mathbf{P}\mathbf{e} \le \frac{1}{\mu_1}\mathbf{T}_{\mathrm{d}}^{\mathrm{T}}\mathbf{Q}_1\mathbf{T}_{\mathrm{d}}^{\mathrm{T}} + \mu_1(\mathbf{P}\mathbf{e})^{\mathrm{T}}\mathbf{Q}_1^{-1}(\mathbf{P}\mathbf{e}) \tag{21}$$

$$2\tilde{\mathbf{f}}_{\mathrm{a}}^{\mathrm{T}}\mathbf{G}^{-1}\dot{\mathbf{f}}_{\mathrm{a}} \le \frac{1}{\mu_2}\tilde{\mathbf{f}}_{\mathrm{a}}^{\mathrm{T}}\mathbf{Q}_2\tilde{\mathbf{f}}_{\mathrm{a}}^{\mathrm{T}} + \mu_2\left(\mathbf{G}^{-1}\dot{\mathbf{f}}_{\mathrm{a}}\right)^{\mathrm{T}}\mathbf{Q}_2^{-1}\left(\mathbf{G}^{-1}\dot{\mathbf{f}}_{\mathrm{a}}\right) \tag{22}$$

$$2\tilde{\mathbf{f}}_{\mathrm{a}}^{\mathrm{T}}\mathbf{G}^{-1}\mathbf{TG}\hat{\mathbf{f}}_{\mathrm{a}} \le -2\tilde{\mathbf{f}}_{\mathrm{a}}^{\mathrm{T}}\mathbf{G}^{-1}\mathbf{TG}\tilde{\mathbf{f}}_{\mathrm{a}} + \frac{1}{\mu_3}\tilde{\mathbf{f}}_{\mathrm{a}}^{\mathrm{T}}\mathbf{Q}_3\tilde{\mathbf{f}}_{\mathrm{a}} + \mu_3\left(\mathbf{G}^{-1}\mathbf{TG}\mathbf{f}_{\mathrm{a}}\right)^{\mathrm{T}}\mathbf{Q}_3^{-1}\left(\mathbf{G}^{-1}\mathbf{TG}\mathbf{f}_{\mathrm{a}}\right) \tag{23}$$

To simplify the calculation, define the following transformation:

$$\boldsymbol{\upsilon} = \begin{bmatrix}\mathbf{e}^{\mathrm{T}} & \tilde{\mathbf{f}}_{\mathrm{a}}^{\mathrm{T}}\end{bmatrix}^{\mathrm{T}} \tag{24}$$

$$\theta = \frac{1}{\mu_1}\mathbf{T}_{\mathrm{d}}^{\mathrm{T}}\mathbf{Q}_1\mathbf{T}_{\mathrm{d}}^{\mathrm{T}} + \mu_2\left(\mathbf{G}^{-1}\dot{\mathbf{f}}_{\mathrm{a}}\right)^{\mathrm{T}}\mathbf{Q}_2^{-1}\left(\mathbf{G}^{-1}\dot{\mathbf{f}}_{\mathrm{a}}\right) + \mu_3\left(\mathbf{G}^{-1}\mathbf{TG}\mathbf{f}_{\mathrm{a}}\right)^{\mathrm{T}}\mathbf{Q}_3^{-1}\left(\mathbf{G}^{-1}\mathbf{TG}\mathbf{f}_{\mathrm{a}}\right) \tag{25}$$

$$\mathbf{E} = \begin{bmatrix}(-\mathbf{LC})^{\mathrm{T}}\mathbf{P} + \mathbf{P}(-\mathbf{LC}) + r^2\mathbf{P}\mathbf{P} + \mathbf{I} + \mu_1\mathbf{P}\mathbf{Q}_1^{-1}\mathbf{P} & \\ & \frac{1}{\mu_2}\mathbf{Q}_2 + \frac{1}{\mu_3}\mathbf{Q}_3 - 2\mathbf{G}^{-1}\mathbf{TG}\end{bmatrix} \tag{26}$$

Substituting (21)-(26) into (20), we can obtain that:

$$\dot{V} \le \boldsymbol{\upsilon}^{\mathrm{T}}\mathbf{E}\boldsymbol{\upsilon} + \theta \tag{27}$$

When $\mathbf{E} < 0$, we can obtain that $\dot{V} \le -\zeta\left\|\boldsymbol{\upsilon}\right\|^2 + \theta$, where $\zeta = \lambda_{\min}(-\mathbf{E})$, It means that $\dot{V} \le 0$ as long as $\left\|\boldsymbol{\upsilon}\right\|^2 \ge \frac{\theta}{\zeta}$. According to Lyapunov stability theory, $\left(\mathbf{e}, \tilde{\mathbf{f}}_{\mathrm{a}}\right)$ converges to a small set. That is to say, state estimation error and fault estimation error are uniformly bounded. This is the end of proof.

4. Simulation

In this section, numerical simulations are presented to illustrate the feasibility of the proposed fault identification scheme. Four reaction flywheels and magnetorquer are used to provide control moments. Without loss of generality, simulations just consider faults of the single flywheel installed on y-axis and magnetorquer. The satellite inertia matrix and flywheel inertia are as follows:

$$\mathbf{J}=\begin{bmatrix}0.5786 & 0.0003 & 0.0073\\ 0.0003 & 0.5810 & 0.0003\\ 0.0073 & 0.0003 & 0.2383\end{bmatrix} kg\cdot m^2 \quad J_{\mathrm{w}}=1.882e-6 kg\cdot m^2$$

The two observers design parameters of fault identification scheme are showed in Table 2. To illustrate the performance of the scheme, three fault scenarios are given in Table 3, where f_{y} denotes the y-axis fault torque of magnetorquer.

Table 2. Observers design parameters.

parameter	value
L_1	1.45
τ_1	0.4705
τ_2	3.764e-15
ν_{f}	1e-9
$\mathbf{L}_2$	diag([1.093,1.093,1.093])
G	diag([0.08,0.11,0.01])
T	diag([0.01,0.01,0.01])

Table 3. Specification of actuators failure scenarios.

Scenario	Parameter	Time of failure(s)
Scenario 1(S1)	k=0.5,v=10^{-9};f_{y}=-10^{-6}Nm	t>20;t>20
Scenario 2(S2)	k=0,v=5×10^{-9};f_{y}=$e^{t/100}$×10^{-8}Nm	t>20;t>20
Scenario 3(S3)	k=0,v=2×10^{-10};f_{y}=-10^{-6}Nm	t>20;40<t<60,100<t<120

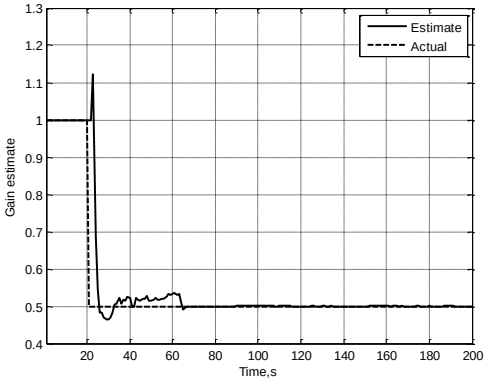

Figure 2. Gain estimate (S1).

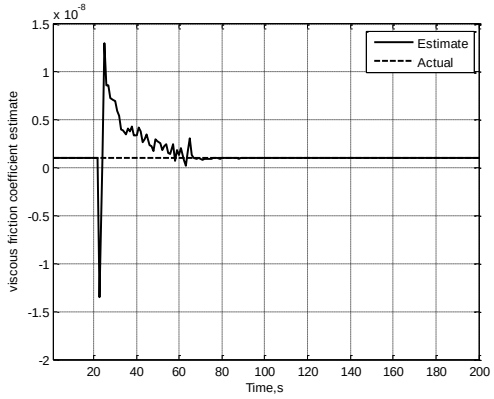

Figure 3. Viscous friction coefficient estimate (S1).

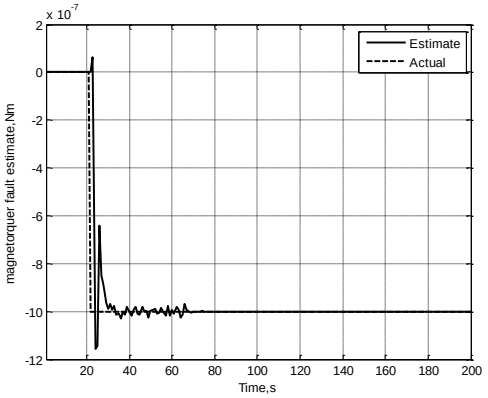

Figure 4. Magnetorquer fault estimate (S1).

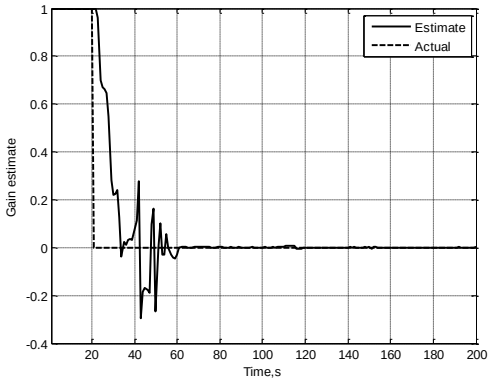

Figure 5. Gain estimate (S2).

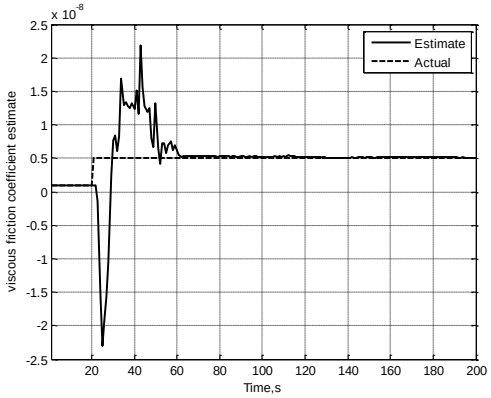

Figure 6. Viscous friction coefficient estimate (S2).

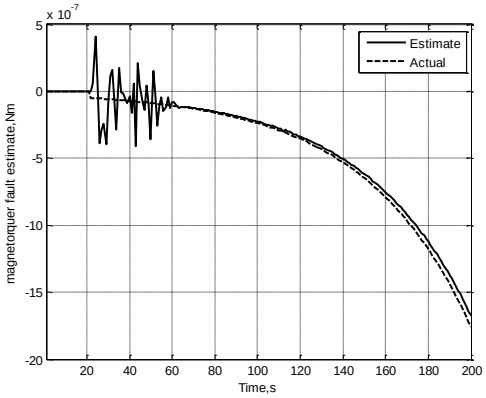

Figure 7. Magnetorquer fault estimate (S2).

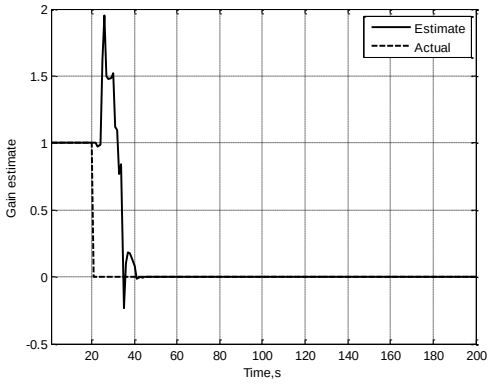

Figure 8. Gain estimate (S3).

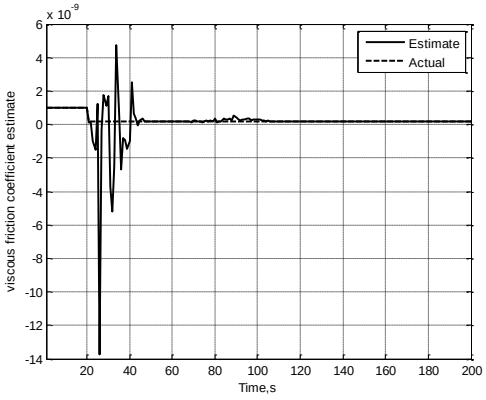

Figure 9. Viscous friction coefficient estimate (S3).

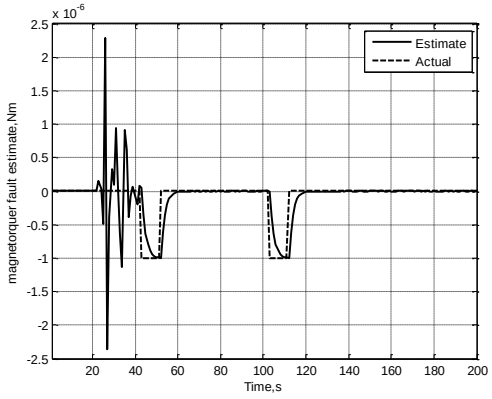

Figure 10. Magnetorquer fault estimate (S3).

In scenario 1, the gain decrease fault of the flywheel and the bias fault of the magnetorquer occur at 21s. The dashed line denotes the actual value and the solid line represents the estimated value. As shown in Fig.2 and Fig.3, the local observer can estimate output gain and viscous friction coefficient accurately within 40 seconds. It can be noted from Tab.1 that the flywheel occurred gain decrease fault, which is consistent with the actual fault. Given the global observer has removed flywheel fault torque, it can be seen from Fig.4 that magnetorquer fault is bias fault, and its magnitude is about -10^{-6}Nm.

In scenario 2, both flywheel and magnetorquer malfunction at 21s. It can draw from Fig.5 and Fig.6 that flywheel output gain is about 0 and viscous friction coefficient is about 5×10^{-9}. So the fault mode

of flywheel is stalling fault referring to Tab.1. It can be seen from Fig.7 that the estimated fault torque gradually increase, in other words, magnetorquer occurs slow variation fault.

In scenario 3, the estimated output gain is about 0 and the estimated viscous friction coefficient is about 2×10^{-10} in Fig.8 and Fig.9, which indicates that the flywheel occurs idling fault. It can be seen from Fig.10 that fault magnitude is up to -10^{-6}Nm during 40s~60s and 100s~120s, which shows the fault mode of magnetorquer is intermittent fault.

5. Conclusions

In this Note, an algorithm for adaptive identification of actuator faults in double observers is proposed. The parameterized description of flywheel faults is established. Using the flywheel speed information, the local adaptive observer can identify the flywheel parameters and realize fault identification. The global observer is designed based on the satellite dynamics model. The estimated output torque of flywheel is taken as the input information of global observer, which aims at eliminating the influence of the flywheel fault on the global observer, thereby fault identification of the magnetorquer can be realized. Simulation results demonstrate the effectiveness of the proposed scheme.

References

[1] Wen X, Zhang X W, Qin Y Q 2014 Statistics and analysis of on-orbit failure modes of foreign spacecraft *Quality and reliability*. 13-18.
[2] Tan C L, Hu T B, Wang D P 2011 Analysis on foreign spacecraft in-orbit failures *Spacecraft Engineering*.
[3] Wen J J, Huang D 2007 Review on fault diagnosis *Advances in Computer Technology and Applications*.
[4] Xie M, Lou X 2016 Reviewed and developing trend of spacecraft fault diagnosis technology *Software*. **37(7)** 70-74.
[5] Su L, Shang C X, Liu W J 2010 Survey on the technology of fault diagnosis for spacecraft attitude control system *Journal of Changchun University of Science and Technology*, **33(4)**:23-27.
[6] Zhu S, Wang D, Shen Q 2017 Satellite attitude stabilization control with actuator faults *Journal of Guidance, Control, and Dynamics*. 1-11.
[7] Lu W G, Su Z H, Qi J 2018 Method of satellite fault diagnosis based on wavelet transform *Foreign Electronic Measurement Technology*.
[8] Gueddi I, Nasri O, Benothman K 2017 Fault detection and isolation of spacecraft thrusters using an extended principal component analysis to interval data *International Journal of Control Automation & Systems*. **15(2)** 1-14.
[9] Gueddi I, Nasri O, Benothman K 2015 VPCA-based fault diagnosis of spacecraft reaction wheels *2015 XXV International Conference on Information, Communication and Automation Technologies*.
[10] Su Z H, Lu W G, Qi J 2016 A method of satellite fault diagnosis based on BP neural network *Computer Measurement & Control*.
[11] Baldi P, Blanke M, Castaldi P 2015 Combined geometric and neural network approach to generic fault diagnosis in satellite reaction wheels *IFAC Papers On Line.* **48(21)** 194-199.
[12] Gao C Y 2013 Model-based actuator fault diagnosis and its application to satellite attitude control systems Harbin. 24-25.
[13] Jiang B, Marcel S 2002 Adaptive observer design for robust fault estimation *International Journal of Systems Science*. **33(9)** 9.
[14] Meng L Y, Jiang B 2008 Fault diagnosis based on the nonlinear adaptive observer *Systems Engineering and Electronics*. **30(7)** 1317-19.